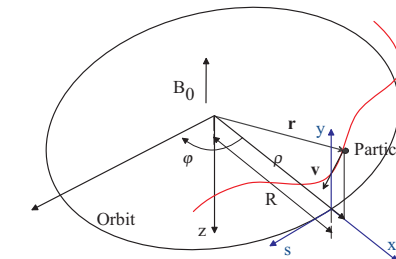


## ACCELERATOR MAGNETS

Stephan Russenschuck

CERN, AT-MEL-EM

1211 Geneva 23, Switzerland

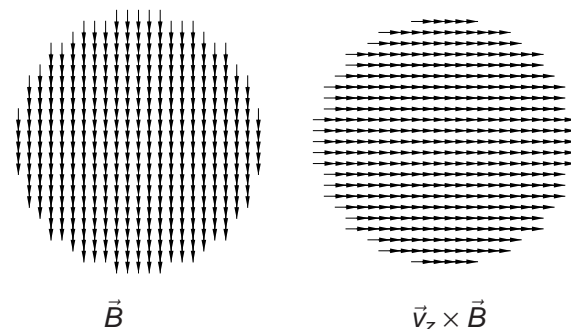


Displaced particle at  $\rho = R + x$  with field  $B_z = B_0 + \frac{\partial B_z}{\partial x} \Big|_{x=0} x$

$$\frac{1}{p_0 ds} \left( p_0 \frac{dx}{ds} \right) + \left( \frac{1}{R^2} - k \right) x = 0$$

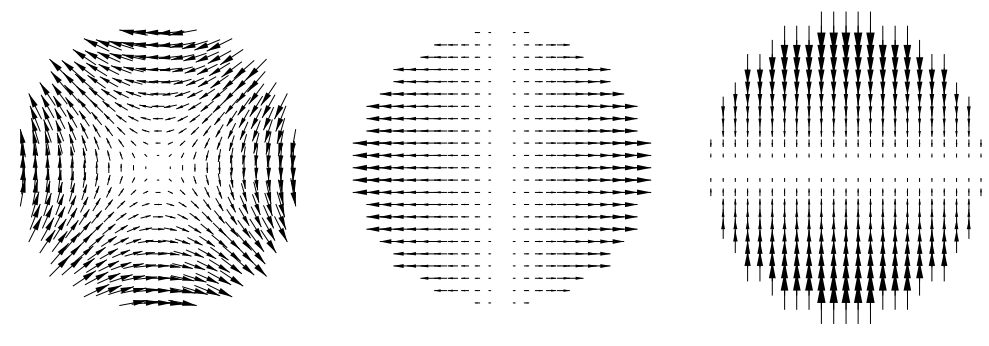
For  $x \ll R$ ,  $e/p_0 = -1/(B_0 R)$  and  $k = -\frac{1}{B_0 R} \frac{\partial B_z}{\partial x} \Big|_{x=0}$

## Bending Field (Dipole) and Magnetic Rigidity



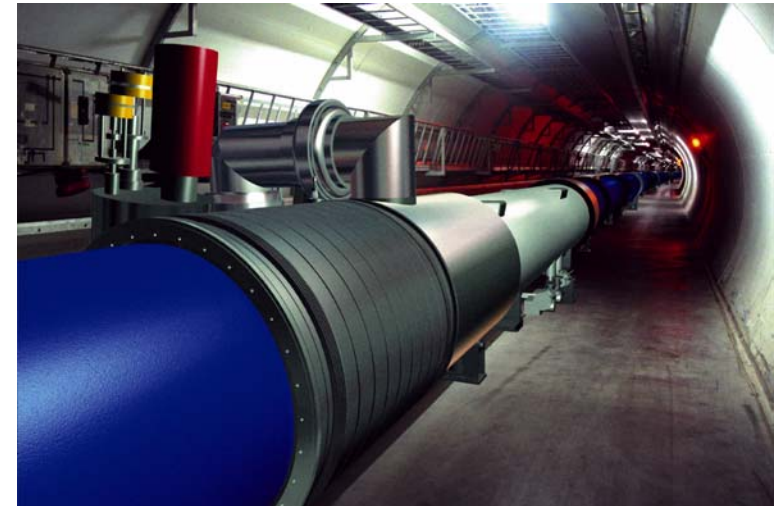
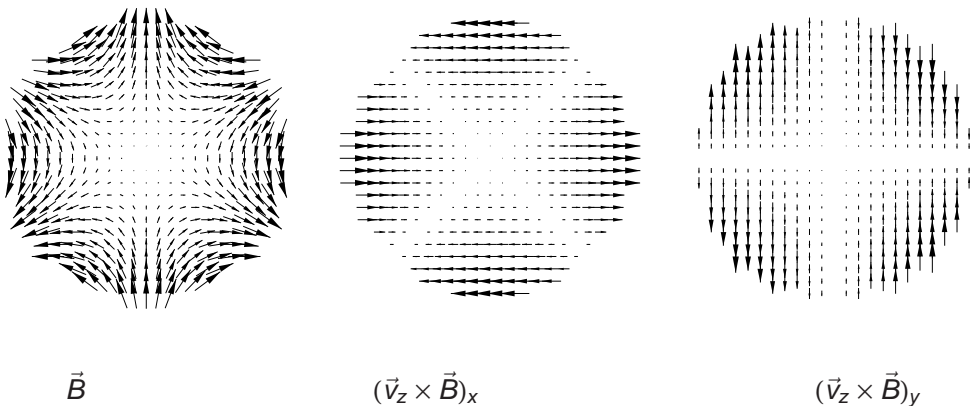
$$3.3356 p[\text{GeV}/c] = R[\text{m}] B_0[\text{T}]$$

## Quadrupole



Remark 1: Consider the “filling factor” in accelerators between 0.6 and 0.7.

## Higher Order Multipole Fields: Sextupole



Remark 2: Magnet systems are the most costly item in an accelerator

## Multipole Field Errors and Beam Parameters

$b_1, a_1$	Closed orbit distortions
$b_2$	$\beta$ -beating
$a_2$	Vertical dispersion, linear coupling
$b_3$	Off-momentum $\beta$ beating
$a_3$	Chromatic coupling inducing detuning
$b_4$	Dynamic aperture and detuning
$a_4$	Dynamic aperture at injection
$b_5$	Dynamic aperture and detuning
$a_5$	Off-momentum dynamic aperture
$b_7$	Dynamic aperture at injection
$b_6, a_6, a_7, >$	Dynamic aperture at injection

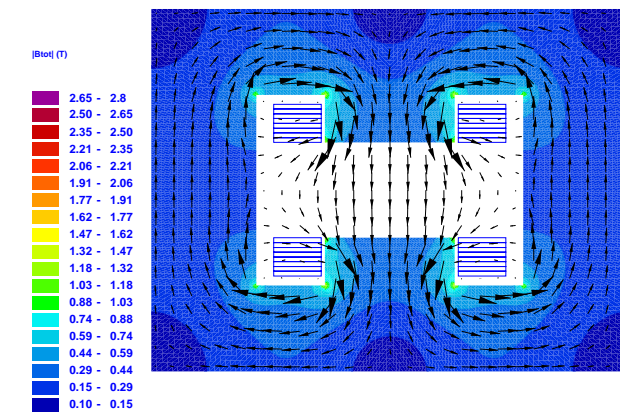
## The 26 GeV Proton Synchrotron (PS) in its Tunnel



## High Energy Ring Accelerator (HERA) at DESY

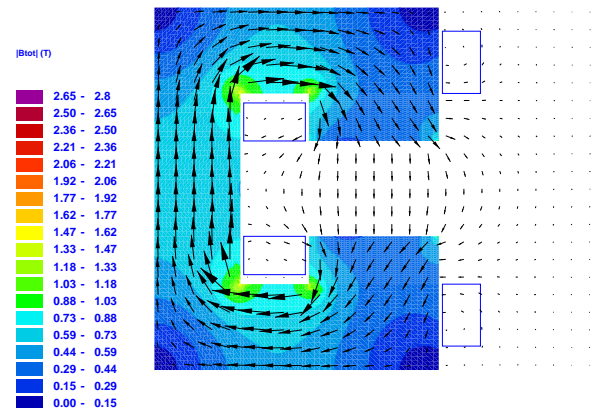


## Magnet Metamorphosis (H-Magnet)



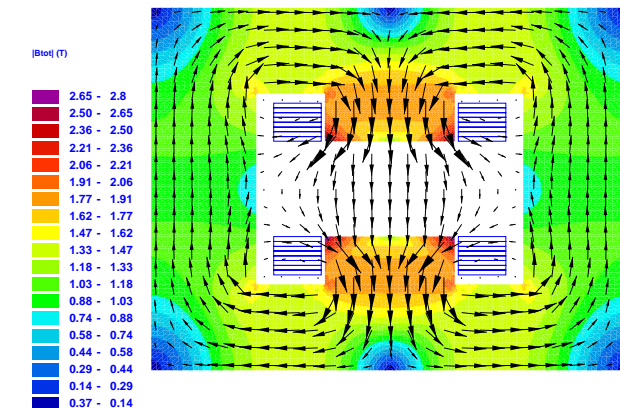
$$N \cdot I = 24000 \text{ A} \quad B_1 = 0.3 \text{ T} \quad B_s = 0.065 \text{ T} \quad \text{Fill.fac. } 0.98$$

## Magnet Metamorphosis (C- Core, LEP Dipole)



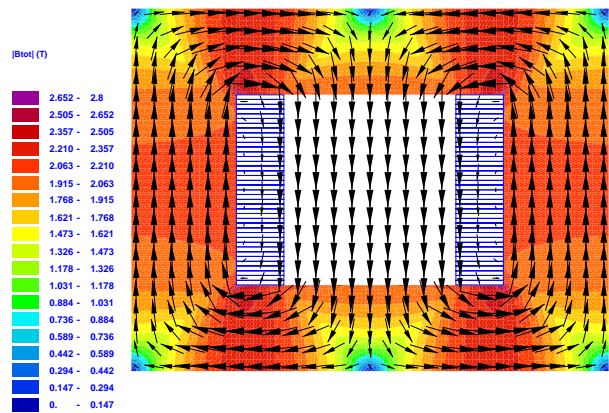
$$N \cdot I = 4480 \text{ A} \quad B_1 = 0.13 \text{ T} \quad B_s = 0.042 \text{ T} \quad \text{Fill.fac. } 0.27$$

## Magnet Metamorphosis (Cryogenic or Super-Ferric Magnet)



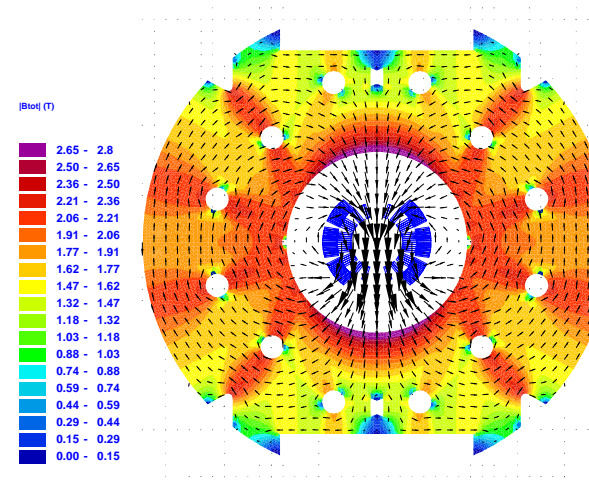
$$N \cdot I = 96000 \text{ A} \quad B_1 = 1.18 \text{ T} \quad B_s = 0.26 \text{ T}$$

## Magnet Metamorphosis (Window Frame Dipole)



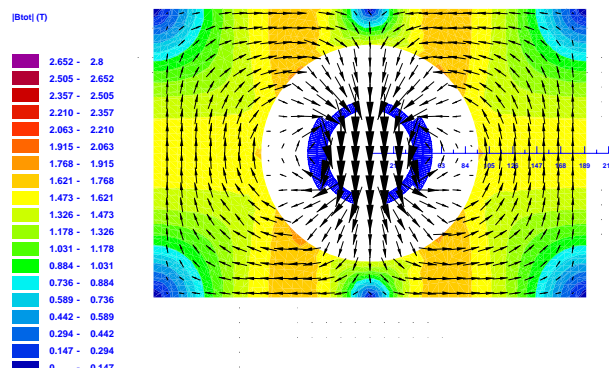
$$N \cdot I = 360000 \text{ A} \quad B_1 = 2.08 \text{ T} \quad B_s = 1.04 \text{ T}$$

## Magnet Metamorphosis (LHC Coil-Test Facility)



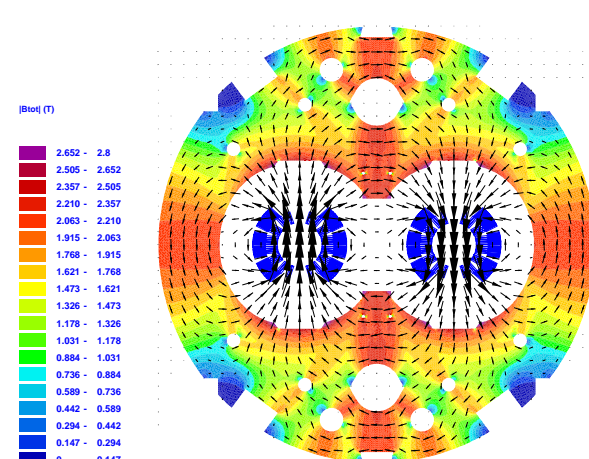
$$N \cdot I = 960000 \text{ A} \quad B_1 = 8.33 \text{ T} \quad B_s = 7.77 \text{ T}$$

## Magnet Metamorphosis (Tevatron Dipole)



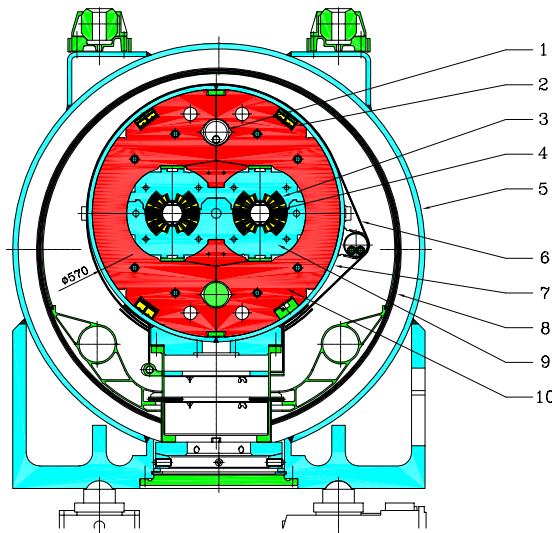
$$N \cdot I = 471000 \text{ A} \quad B_1 = 4.16 \text{ T} \quad B_s = 3.39 \text{ T}$$

## Magnet Metamorphosis (LHC Main Dipole)



$$N \cdot I = 2x944000 \text{ A} \quad B_1 = 8.32 \text{ T} \quad B_s = 7.44 \text{ T}$$

## LHC Main Dipol Cross-Section



1. Heat exchanger, 2. Bus bar, 3. Superconducting coil, 4. Vacuum Pipe und Beam-screen, 5. Cryostat,  
6. Thermal shield (55- 75 K), 7. Helium-Tank, 8. Super-Insulation, 9. Collars, 10. Yoke

## Maxwell's Equations in Integral Form

$$\oint \vec{H} \cdot d\vec{s} = \int_A (\vec{J} + \frac{\partial \vec{D}}{\partial t}) \cdot d\vec{A}$$

$$\oint \vec{E} \cdot d\vec{s} = -\frac{\partial}{\partial t} \int_A \vec{B} \cdot d\vec{A}$$

$$\int_A \vec{B} \cdot d\vec{A} = 0$$

$$\int_A \vec{D} \cdot d\vec{A} = \int_V \rho dV$$

## Constitutive Equations

$$\vec{B} = \mu \vec{H} = \mu_0(\vec{H} + \vec{M})$$

$$\vec{D} = \epsilon \vec{E} = \epsilon_0(\vec{E} + \vec{P})$$

$$\vec{J} = \kappa \vec{E} + J_{\text{imp.}}$$

## Overview

**Maxwell's equations in integral form**  
One-dimensional field calculation for conventional magnets

**Maxwell's equations in differential form**

The solution of Laplace's equation

Harmonic fields

**Complex Potentials**

Ideal pole shapes of conventional magnets

Feed down

**Solution of Poisson's equation**

The field of line currents

Generation of pure multipole fields

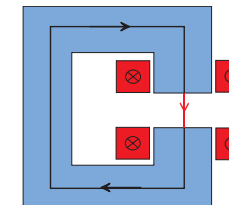
Sensitivity to manufacturing errors

**Numerical field computation**

Saturation of the iron yoke

Superconducting filament magnetization

## 1D Field Calculation for a Conventional Dipole



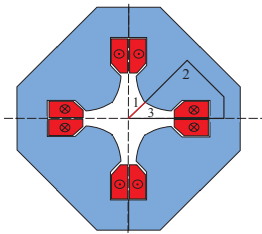
$$\oint \vec{H} \cdot d\vec{s} = \int_A \vec{J} \cdot d\vec{A}$$

$$H_{\text{iron}} s_{\text{iron}} + H_{\text{gap}} s_{\text{gap}} = \frac{1}{\mu_0 \mu_r} B_{\text{iron}} s_{\text{iron}} + \frac{1}{\mu_0} B_{\text{gap}} s_{\text{gap}} = N I$$

$$\mu_r \gg 1 \quad B_{\text{gap}} = \frac{\mu_0 N I}{s_{\text{gap}}}$$

**Warning 1:** Check that the magnetic circuit contains no flux concentration which increases the magnetic flux density above 1 T, as in this case fringe fields can no longer be neglected.

## 1D Field Calculation for a Conventional Quadrupole

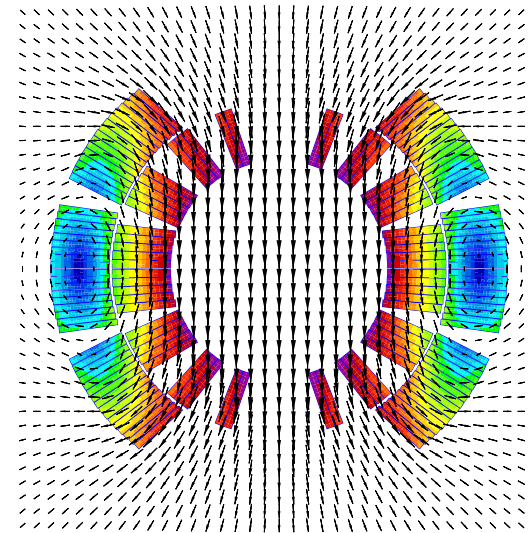


$$\oint \vec{H} \cdot d\vec{s} = \int_1 \vec{H}_1 \cdot d\vec{s} + \int_2 \vec{H}_2 \cdot d\vec{s} + \int_3 \vec{H}_3 \cdot d\vec{s} = NI$$

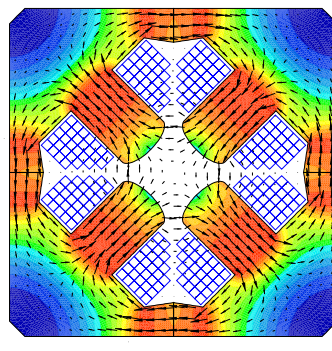
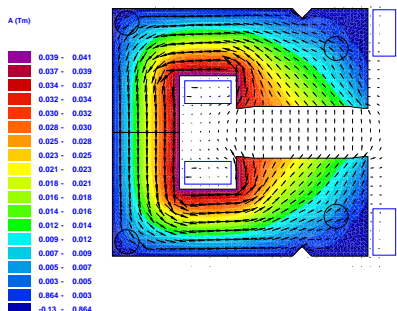
$$B_x = gy \quad B_y = gx \quad \Rightarrow \quad H = \frac{g}{\mu_0} \sqrt{x^2 + y^2} = \frac{g}{\mu_0} r$$

$$\int_0^{r_0} H dr = \frac{g}{\mu_0} \int_0^{r_0} r dr = \frac{g}{\mu_0} \frac{r_0^2}{2} = NI \quad \Rightarrow \quad g = \frac{2\mu_0 NI}{r_0^2}$$

## Field Quality in the Dipole Aperture

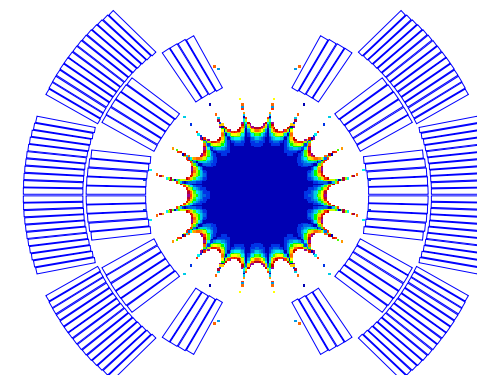


## LEP Dipole and Quadrupole



## Field Quality in the Dipole Aperture

$$|1 - \frac{B_y}{B_y^{\text{nom}}}|$$



## Definition of Field Quality in Accelerator Magnets

Fourier-series expansion of the **radial component of the magnetic flux density**  
on a reference radius **inside** the aperture

$$\begin{aligned} B_r(r_0, \varphi) &= \sum_{n=1}^{\infty} (B_n(r_0) \sin n\varphi + A_n(r_0) \cos n\varphi) \\ &= B_N(r_0) \sum_{n=1}^{\infty} (\textcolor{blue}{b}_n(r_0) \sin n\varphi + \textcolor{blue}{a}_n(r_0) \cos n\varphi) \end{aligned}$$

$$A_n(r_0) \approx \frac{1}{P} \sum_{k=0}^{2P-1} B_r(r_0, \varphi_k) \cos n\varphi_k, \quad B_n(r_0) \approx \frac{1}{P} \sum_{k=0}^{2P-1} B_r(r_0, \varphi_k) \sin n\varphi_k.$$

**Remark 3:** This definition is perfectly in line with magnetic field measurements using “harmonic coils” where the periodic flux variation in tangential rotating coils is analyzed with a FFT.

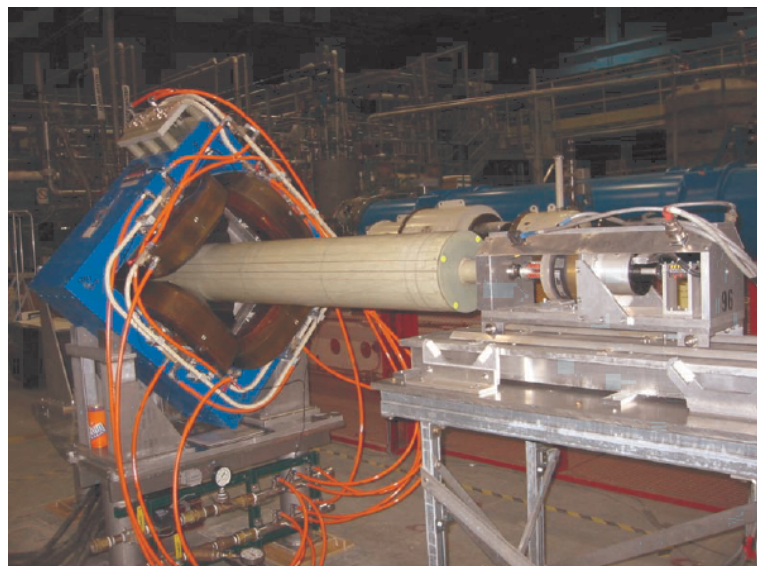
## Maxwell's Equations in Differential Form

$$\begin{aligned} \operatorname{curl} \vec{H} &= \vec{J} + \frac{\partial \vec{D}}{\partial t} \\ \operatorname{curl} \vec{E} &= -\frac{\partial \vec{B}}{\partial t} \\ \operatorname{div} \vec{B} &= 0 \\ \operatorname{div} \vec{D} &= \rho \end{aligned}$$

## Constitutive Equations

$$\begin{aligned} \vec{B} &= \mu \vec{H} = \mu_0 (\vec{H} + \vec{M}) \\ \vec{D} &= \epsilon \vec{E} = \epsilon_0 (\vec{E} + \vec{P}) \\ \vec{J} &= \kappa \vec{E} + J_{\text{imp.}} \end{aligned}$$

## Rotating Coil Measurement Setup at BNL (Brookhaven)



## Lemmata of Poincaré

The curl of an arbitrary vector field is source free  $\operatorname{div} \operatorname{curl} \vec{g} = 0$   
An arbitrary gradient field is curl free  $\operatorname{curl} \operatorname{grad} \phi = 0$

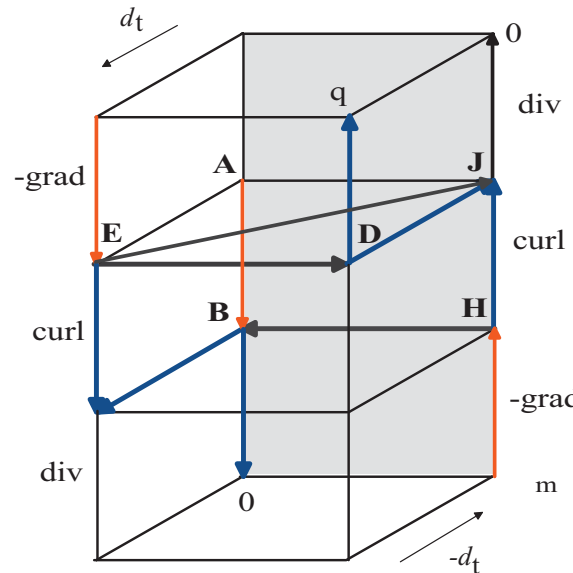
A source free field  $\vec{B}$ , ( $\operatorname{div} \vec{B} = 0$ )  
can be expressed through a vector potential  $\vec{A}$  in the form  
 $\vec{B} = \operatorname{curl} \vec{A}$ .

A curl free field  $\vec{H}$ , ( $\operatorname{curl} \vec{H} = 0$ )  
can be expressed through a scalar potential  $\phi$  in the form  $\vec{H} = -\operatorname{grad} \Phi_m$ .

**Remark 4:** The field in the aperture of accelerator magnets  
is curl **and** source free

**Warning 2:** The Lemmata of Poincaré hold only for simply connected domains with connected boundaries.

## Maxwell's "House"



## General Solution of the Laplace Equation

$$A_z(r, \varphi) = \sum_{n=1}^{\infty} (E_n r^n + F_n r^{-n}) (G_n \sin n\varphi + H_n \cos n\varphi)$$

$$B_r(r, \varphi) = \frac{1}{r} \frac{\partial A_z}{\partial \varphi} = \sum_{n=1}^{\infty} n r^{n-1} (C_n \sin n\varphi + D_n \cos n\varphi)$$

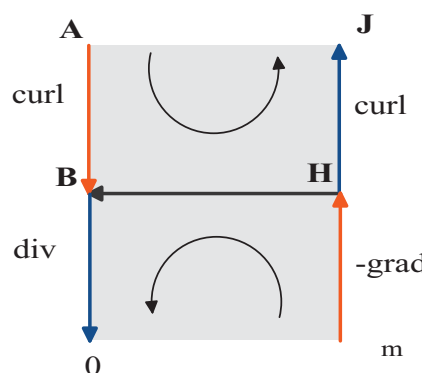
$$n r^{n-1} C_n = B_n \quad n r^{n-1} D_n = A_n$$

$$B_\varphi(r, \varphi) = -\frac{\partial A_z}{\partial r} = -\sum_{n=1}^{\infty} n r^{n-1} (D_n \sin n\varphi - C_n \cos n\varphi)$$

**Warning 3:** Only for sub-domains with continuous material parameters.

## Maxwell's "Facade"

$$\operatorname{curl} \frac{1}{\mu} \operatorname{curl} \vec{A} = \vec{J} \quad \frac{1}{\mu_0} \operatorname{curl} \operatorname{curl} \vec{A} = 0 \quad \nabla^2 \vec{A} - \operatorname{grad} \operatorname{div} \vec{A} = 0 \quad \nabla^2 A_z = 0$$



$$\operatorname{div} \mu \operatorname{grad} \Phi_m = 0 \quad \mu_0 \operatorname{div} \operatorname{grad} \Phi_m = 0 \quad \nabla^2 \Phi_m = 0$$

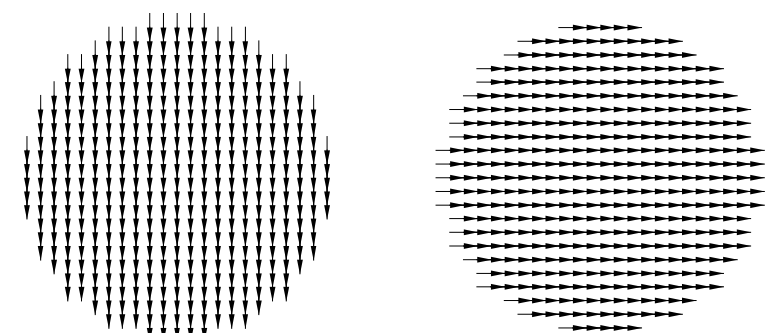
$$r^2 \frac{\partial^2 A_z}{\partial r^2} + r \frac{\partial A_z}{\partial r} + \frac{\partial^2 A_z}{\partial \varphi^2} = 0$$

### Normal (Skew) Dipole (n=1)

$$B_r = C_1 \cos \varphi + D_1 \sin \varphi \quad B_\varphi = -C_1 \sin \varphi + D_1 \cos \varphi$$

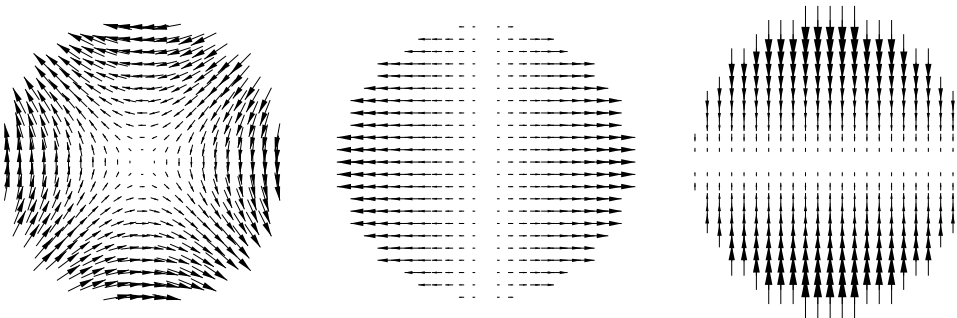
$$B_x = B_r \cos \varphi - B_\varphi \sin \varphi \quad B_y = B_r \sin \varphi + B_\varphi \cos \varphi$$

$$B_x = C_1 \quad B_y = D_1$$



### Normal (Skew) Quadrupole (n=2)

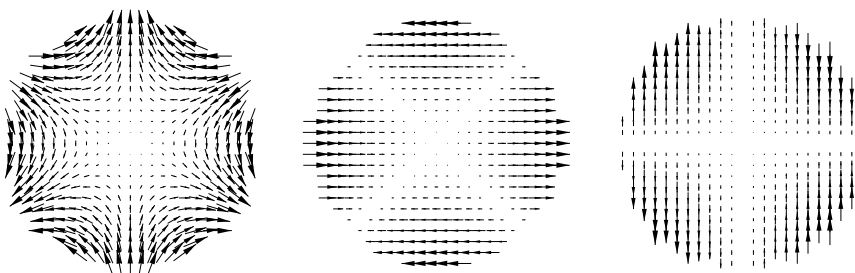
$$\begin{aligned}B_r &= 2C_2 r \cos 2\varphi + 2D_2 r \sin 2\varphi \\B_\varphi &= -2C_2 r \sin 2\varphi + 2D_2 r \cos 2\varphi \\B_x &= 2C_2 x + 2D_2 y \\B_y &= -2C_2 y + 2D_2 x\end{aligned}$$



**Remark 5:** Notice that we have not yet addressed the problem of how to create such field distributions.

### Normal (Skew) Sextupole (n=3)

$$\begin{aligned}B_r &= 3C_3 r^2 \cos 3\varphi + 3D_3 r^2 \sin 3\varphi \\B_\varphi &= -3C_3 r^2 \sin 3\varphi + 3D_3 r^2 \cos 3\varphi \\B_x &= 3C_3(x^2 - y^2) + 6D_3 xy \\B_y &= -6C_3 xy + 3D_3(x^2 - y^2)\end{aligned}$$



**Remark 6:** The treatment of each harmonic separately is a mathematical abstraction. In practical situations many harmonics will be present (to be minimized).

## Analytical Field Computation for Superconducting Magnets

Special solution of the inhomogeneous (Poisson) differential equation

$$\nabla^2 \vec{A} = \vec{J}$$

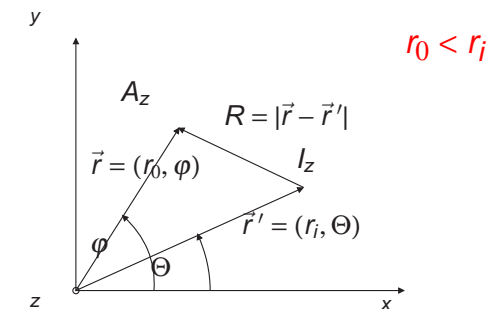
Fundamental solution of the Laplace Operator  $\nabla^2$  (Green's Function)

$$\begin{aligned}(2D) \quad G &= \frac{1}{2\pi} \ln |\vec{r} - \vec{r}'| \\(3D) \quad G &= \frac{1}{4\pi} \frac{1}{|\vec{r} - \vec{r}'|}\end{aligned}$$

Vector potential of a line current (2D)

$$A_z = -\frac{\mu_0 I}{2\pi} \ln \left( \frac{|\vec{r} - \vec{r}'|}{a} \right)$$

The Field of Line Currents (2D)



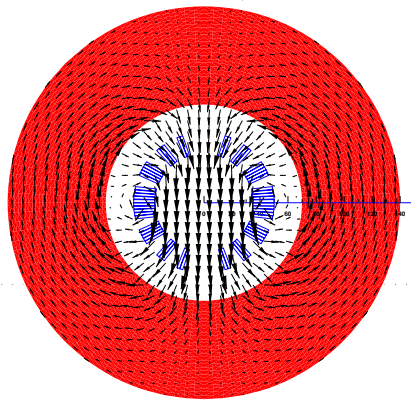
$$A_z = -\frac{\mu_0 I}{2\pi} \ln \left( \frac{|\vec{r} - \vec{r}'|}{a} \right)$$

$$B_r = -\frac{\mu_0 I}{2\pi} \sum_{n=1}^{\infty} \left( \frac{r_0^{n-1}}{r_i^n} \right) (\sin n\varphi \cos n\Theta - \cos n\varphi \sin n\Theta)$$

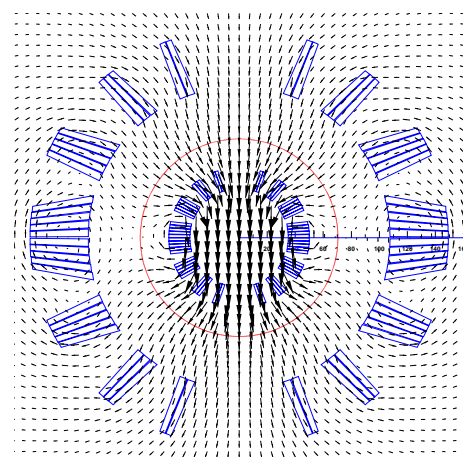
$$B_n(r_0) = -\frac{\mu_0 I r_0^{n-1}}{2\pi r_i^n} \cos n\Theta \quad A_n(r_0) = \frac{\mu_0 I r_0^{n-1}}{2\pi r_i^n} \sin n\Theta$$

## The Imaging Method

Coil in non-saturated yoke



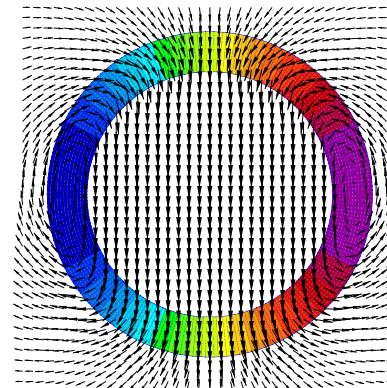
Imaged coil



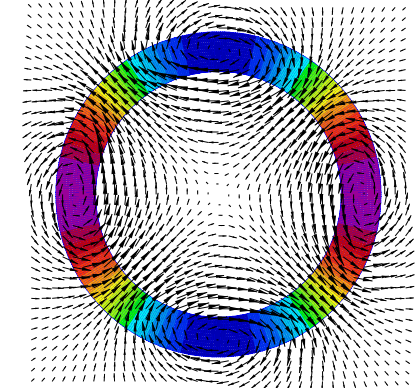
## Ideal ( $\cos n \theta$ ) Current Distribution

$$B_n(r_0) = - \sum_{i=1}^{n_s} \int_{r_i}^{r_o} \int_0^{2\pi} \frac{\mu_0 J_0 \cos m\Theta}{2\pi} r_i^{n-1} \left( 1 + \frac{\mu_r - 1}{\mu_r + 1} \left( \frac{r_i}{R_{Yoke}} \right)^{2n} \right) \cos n\Theta_i r d\Theta dr$$

Dipole



Quadrupole



## Field Harmonics in SC Magnet

$$B_n(r_0) = - \sum_{i=1}^{n_s} \frac{\mu_0 I_i}{2\pi} \frac{r_0^{n-1}}{r_i^n} \left( 1 + \frac{\mu_r - 1}{\mu_r + 1} \left( \frac{r_i}{R_{Yoke}} \right)^{2n} \right) \cos n\Theta_i$$

Scaling laws

$$B_n(r_1) = (r_1/r_0)^{n-1} B_n(r_0)$$

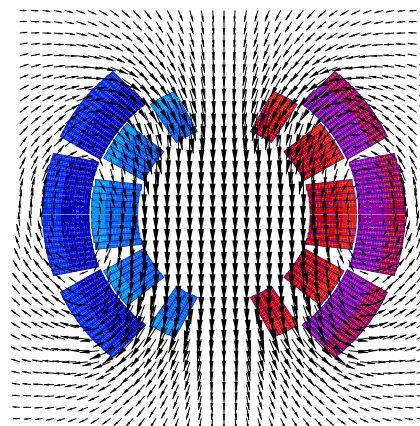
Influence of the iron yoke (non-saturated)

$$r_i = 43.5 \text{ mm}, R_{Yoke} = 89 \text{ mm}: B_1 - 19\%, B_5 - 0.07\%$$

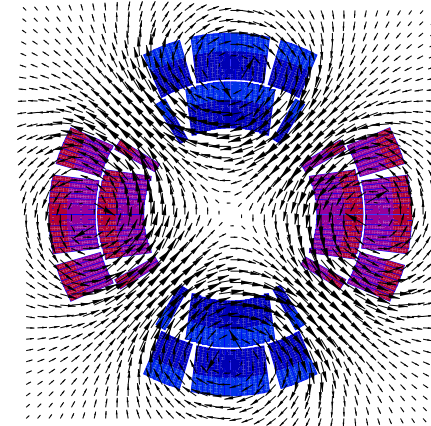
**Remark 7:** Analytical field optimization can be used for higher order harmonics, finite element calculations (for the estimation of saturation effects in the iron yoke) only needed for the lower order harmonics.

## Ideal Current Distribution Approximated with Coil-Blocks

Dipole



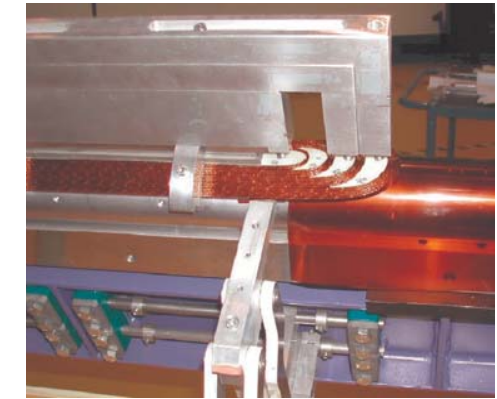
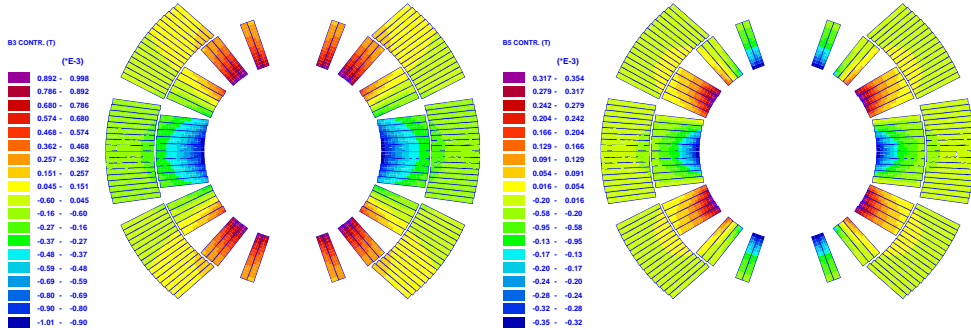
Quadrupole



## Coil Winding

### B<sub>3</sub> and B<sub>5</sub> Contribution of Strand Current

$$B_n(r_0) = -\frac{\mu_0 I_i r_0^{n-1}}{2\pi r_i^n} \left( 1 + \frac{\mu_r - 1}{\mu_r + 1} \left( \frac{r_i}{R_{Yoke}} \right)^{2n} \right) \cos n\Theta_i$$



### Sensitivity to Coil Block Displacements

$$B_n(r_0) = -\frac{\mu_0 I_i r_0^{n-1}}{2\pi r_i^n} \left( 1 + \frac{\mu_r - 1}{\mu_r + 1} \left( \frac{r_i}{R_{Yoke}} \right)^{2n} \right) \cos n\Theta_i$$

$$\frac{\partial B_n(r_0)}{\partial \Theta_i} = -\frac{\mu_0 I_i n r_0^{n-1}}{2\pi r_i^n} \left( 1 + \left( \frac{r_i}{R_{Yoke}} \right)^{2n} \right) \sin n\Theta_i$$

$$\frac{\partial B_n(r_0)}{\partial r_i} = \frac{\mu_0 I_i n r_0^{n-1}}{2\pi r_i^{n+1}} \left( 1 - \left( \frac{r_i}{R_{Yoke}} \right)^{2n} \right) \cos n\Theta_i$$

Increase of the azimuthal coil size by 0.1 mm produces (in units of 10<sup>-4</sup>):

$$b_1 = -14. \quad b_3 = 1.2 \quad b_5 = 0.03$$

Specified tolerances on coils: ± 0.025 mm

### Curing Press and Curing Mold



## Feed down

### Complex Potentials

$$\vec{H} = -\text{grad}\Phi_m = -\frac{\partial\Phi_m}{\partial x}\vec{e}_x - \frac{\partial\Phi_m}{\partial y}\vec{e}_y$$

$$\vec{B} = \text{curl}A_z = \frac{\partial A_z}{\partial y}\vec{e}_x - \frac{\partial A_z}{\partial x}\vec{e}_y$$

### Cauchy-Riemann DEQ

$$\frac{\partial A_z}{\partial y} = -\mu_0 \frac{\partial \Phi_m}{\partial x} \quad \frac{\partial A_z}{\partial x} = \mu_0 \frac{\partial \Phi_m}{\partial y}$$

$$W(z) = A_z(x, y) + i\mu_0\Phi_m(x, y) \quad z = x + iy$$

$$-\frac{dW}{dz} = -\frac{\partial A_z}{\partial x} - i\mu_0 \frac{\partial \Phi_m}{\partial x} = B_y(x, y) + iB_x(x, y)$$

$$\sum_{n=1}^{\infty} c_n \left( \frac{z}{r_0} \right)^{n-1} = \sum_{n=1}^{\infty} c'_n \left( \frac{z'}{r_0} \right)^{n-1} = B_y + i B_x$$

$$z = z' + \Delta z \quad z = x + iy$$

$$c'_n = \sum_{k=n}^{\infty} c_k \frac{(k-1)!}{(k-n)! (n-1)!} \left( \frac{\Delta z}{r_0} \right)^{k-n}$$

$$c'_2 = c_2 + 2 c_3 \left( \frac{\Delta z}{r_0} \right) + 3 c_4 \left( \frac{\Delta z}{r_0} \right)^2 + \dots$$

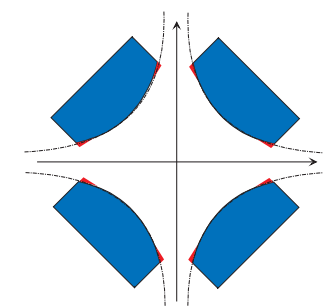
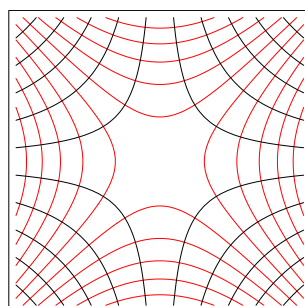
- Measurement of magnetic axis in dipole by powering the coil as a quadrupole.
- The feed down effect can be used to center the measurements coil by minimization of the  $b_{10}$  which can only occur as feed down from  $b_{11}$ .
- The dipole magnetic axis has to be well aligned with respect to the closed orbit:  $\pm 0.1$  mm for both  $\Delta x$  and  $\Delta y$  systematic and 0.5 mm for both  $\sigma_x$  and  $\sigma_y$  random (r.m.s.).
- Alignment tolerances of MCS and MCDO correctors w.r.t. MB: 0.3 mm radially

### Cartesian Field Components

$$W(z) = A_z(x, y) + i\mu_0\Phi_m(x, y) \quad z = x + iy$$

$$B_y + iB_x = \sum_{n=1}^{\infty} (B_n + iA_n) \left( \frac{z_0}{r_0} \right)^{n-1} = -\frac{\mu_0 I}{2\pi} \sum_{n=1}^{\infty} \frac{z_0^{n-1}}{z^n} \quad |z_0| < |z|$$

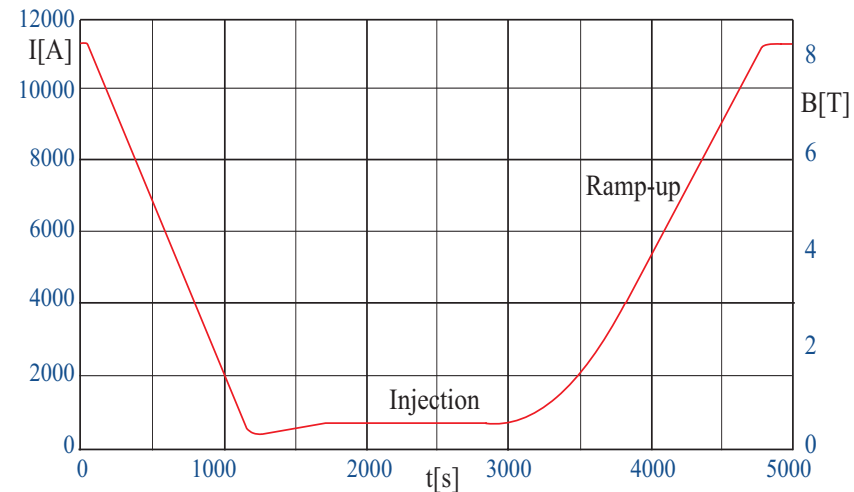
### Ideal (Iron) Pole Shapes



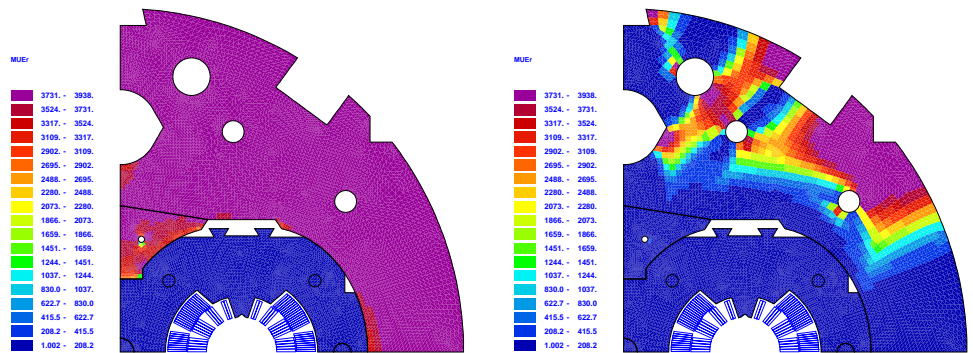
### Mechanical Axis Measurement for Spool Piece Alignment



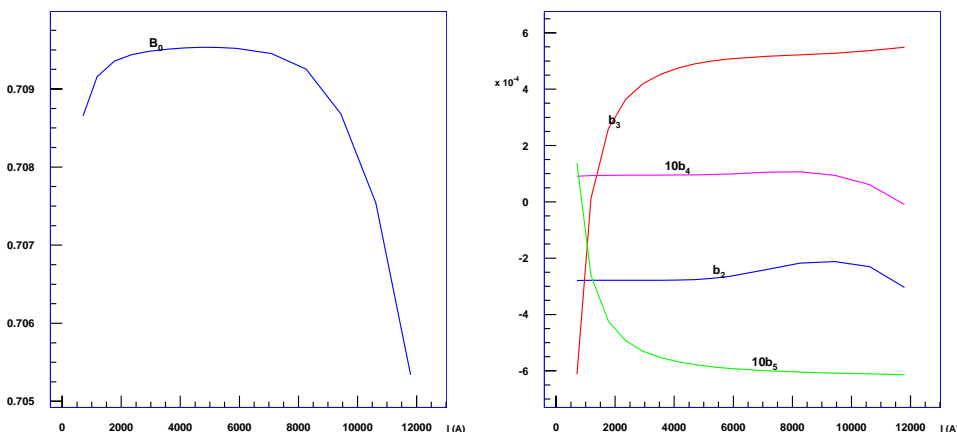
## Excitation Cycle of the LHC Dipoles



## Saturation Effect in LHC Dipoles



## Field Variation with Excitation



## Objectives for the ROXIE Development

Automatic generation of coil geometry

Field computation specially suited for magnet design (BEM-FEM)

No meshing of the coil

No artificial boundary conditions

Confine numerical errors to the iron magnetization

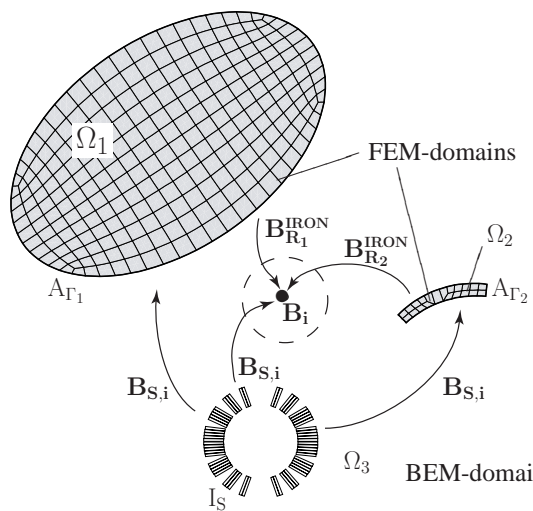
Higher-order quadrilateral finite-elements

Parametric mesh generator

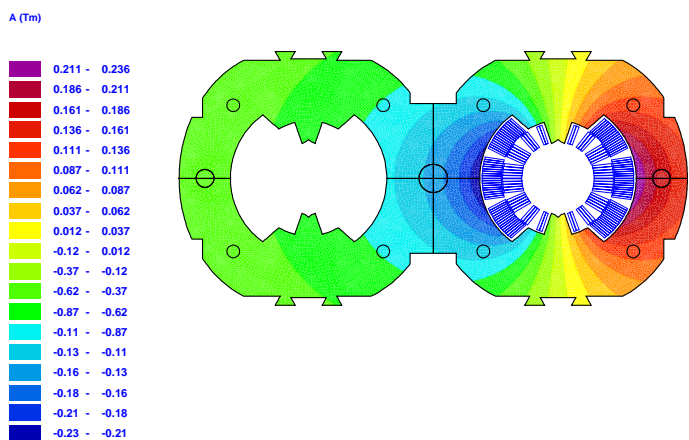
Mathematical optimization

CAD/CAM interfaces

## Field Computation with the BEM-FEM Coupling Method

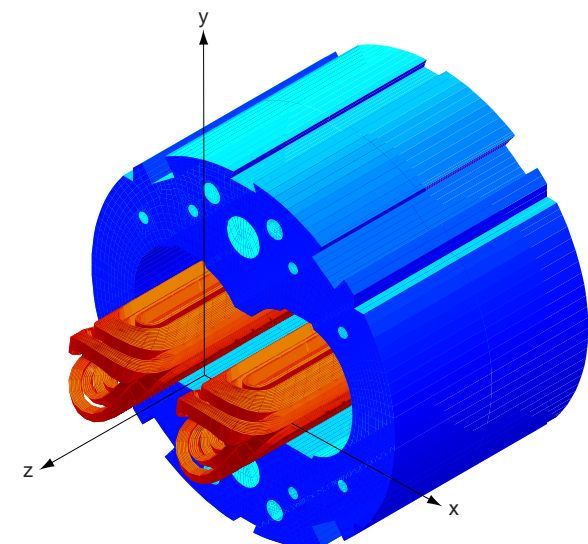


## Field Quality Calculations for Collared Coils



$$b_2 = -0.239 \quad b_3 = 2.742 \quad b_4 = -0.012 \quad b_5 = -0.733$$

## Calculation of Fringe Fields in a LHC Dipole Model



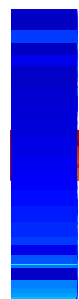
Source field



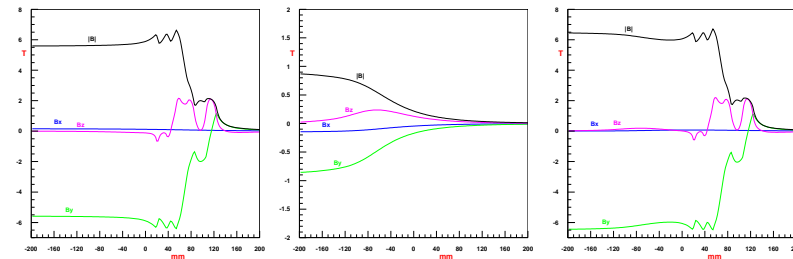
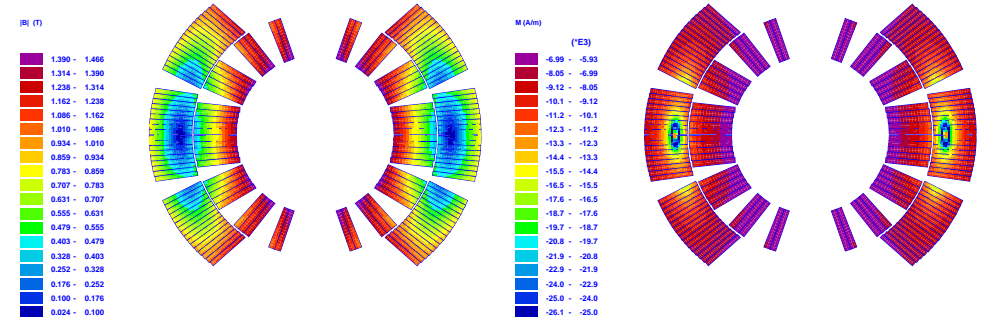
Reduced field



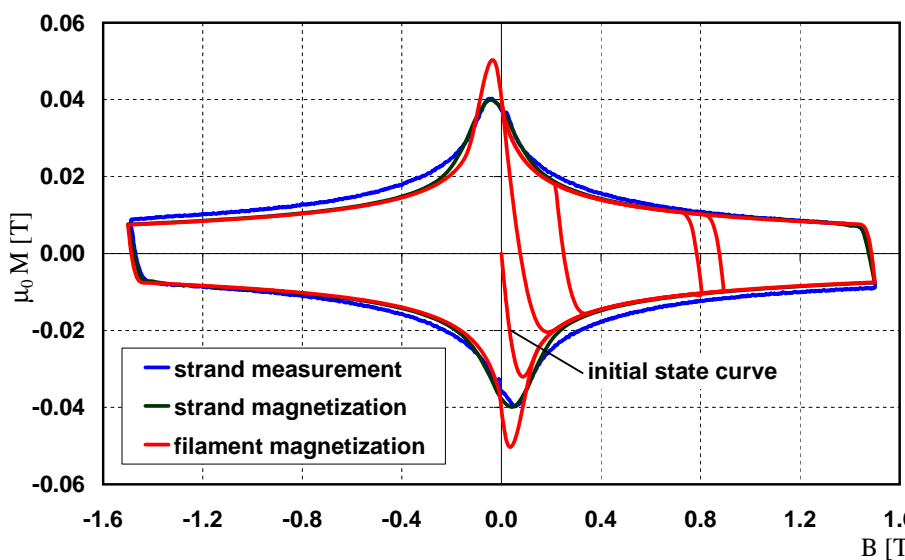
Total field



## Field and Magnetization in the LHC Dipole Coil



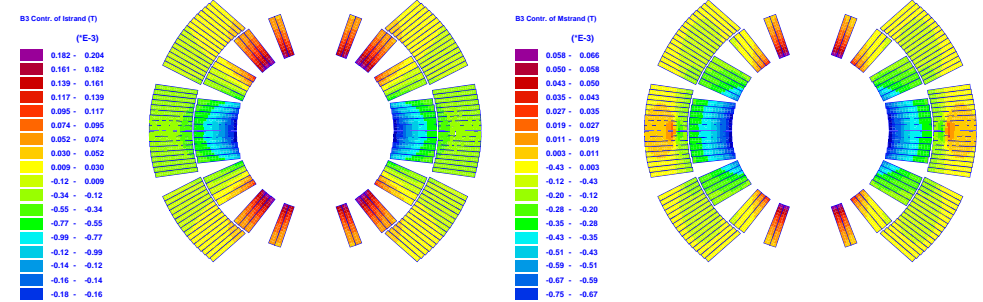
## Hysteresis in Superconductor Magnetization



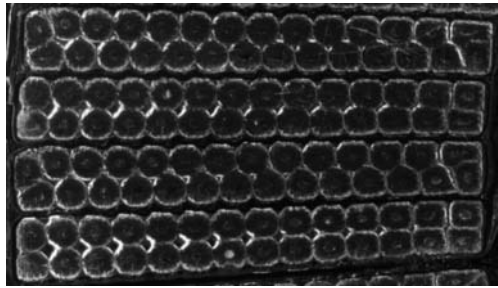
## Generated $B_3$ Field Errors

$$B_n(r_0) = \frac{\mu_0 l_i r_0^{n-1}}{2\pi r_i^n} \cos n\Theta$$

$$B_n(r_0) = \frac{\mu_0 r_0^{n-1}}{2\pi r_i^{n+1}} n(m_{\tilde{r}} \sin n\theta + m_\theta \cos n\theta)$$



## Macro-Photography of Cable and Strand



Inner (outer) layer LHC dipole coil:  
Filament diameter 7 (6)  $\mu\text{m}$ , Strand diameter 1.065 (0.825) mm

## Scaling Laws Hold for Integrated Multipoles

$$\nabla^2 \Phi_m(x, y, z) = \frac{\partial^2 \Phi_m(x, y, z)}{\partial x^2} + \frac{\partial^2 \Phi_m(x, y, z)}{\partial y^2} + \frac{\partial^2 \Phi_m(x, y, z)}{\partial z^2} = 0$$

$$\bar{\Phi}_m(x, y) = \int_{-z_0}^{z_0} \Phi_m(x, y, z) dz$$

$$\nabla^2 \bar{\Phi}_m(x, y) = \frac{\partial^2 \bar{\Phi}_m(x, y)}{\partial x^2} + \frac{\partial^2 \bar{\Phi}_m(x, y)}{\partial y^2} = 0$$

**Sufficient condition:** Integration path is extended far enough away from (into) the magnet so that the axial component of the field has dropped to zero.

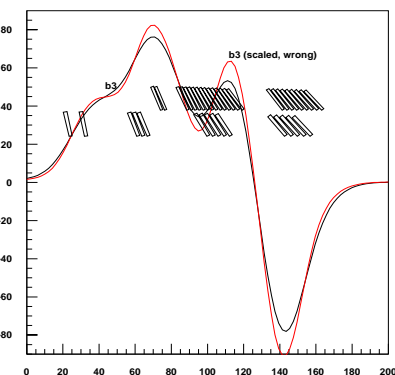
$$\frac{\partial^2 \bar{\Phi}_m}{\partial x^2} + \frac{\partial^2 \bar{\Phi}_m}{\partial y^2} = \int_{-z_0}^{z_0} \left( \frac{\partial^2 \Phi_m}{\partial x^2} + \frac{\partial^2 \Phi_m}{\partial y^2} \right) dz = \int_{-z_0}^{z_0} \left( -\frac{\partial^2 \Phi_m}{\partial z^2} \right) dz = -\left. \frac{\partial \Phi_m}{\partial z} \right|_{-z_0}^{z_0} = H_z|_{-z_0} - H_z|_{z_0}$$

## Warning 4:

### Scaling Laws for Multipoles are Wrong in 3 Dimensions

$$B_n(r_1) = \left(\frac{r_1}{r_0}\right)^{n-1} B_n(r_0)$$

$$b_n(r_1) = \left(\frac{r_1}{r_0}\right)^{n-N} b_n(r_0)$$



### References

- [1] M. Alekса, S. Russenschuck and C. Völlinger *Magnetic Field Calculations Including the Impact of Persistent Currents in Superconducting Filaments* IEEE Trans. on Magn., vol. 38, no. 2, 2002.
- [2] Bossavit, A.: Computational Electromagnetism, Academic Press, 1998
- [3] Beth, R. A.: An Integral Formula for Two-dimensional Fields, Journal of Applied Physics, Vol. 38, Nr. 12, 1967
- [4] Binns, K.J., Lawrenson, P.J., Trowbridge, C.W.: The analytical and numerical solution of electric and magnetic fields, John Wiley & Sons, 1992
- [5] Bryant P.J.: Basic theory of magnetic measurements, CAS, CERN Accelerator School on Magnetic Measurement and Alignment, CERN 92-05, Geneva, 1992
- [6] CAS, CERN Accelerator School on Superconductivity in Particle Accelerators, Haus Rissen, Hamburg, Germany, 1995, Proceedings, CERN-96-03
- [7] Kurz, S., Russenschuck, S.: The application of the BEM-FEM coupling method for the accurate calculation of fields in superconducting magnets, Electrical Engineering, 1999
- [8] Mess, K.H., Schmüser, P., Wolff S.: Superconducting Accelerator Magnets, World Scientific, 1996
- [9] M. Pekeler et al., Coupled Persistent-Current Effects in the Hera Dipoles and Beam Pipe Correction Coils, Desy Report no. 92-06, Hamburg, 1992
- [10] Russenschuck, S.: ROXIE: Routine for the Optimization of magnet X-sections, Inverse field calculation and coil End design, Proceedings of the First International ROXIE users meeting and workshop, CERN 99-01, ISBN 92-9083-140-5.
- [11] Wilson, M.N.: Superconducting Magnets, Oxford Science Publications, 1983